https://doi.org/10.48047/AFJBS.6.7.2024.1991-2002

African Journal of Biological Sciences

Journal homepage: http://www.afjbs.com

Research Paper Open Access

Solar Air Heater Performance Evaluation with Square V-Shaped Ribs on Absorber Plate

Rahul Meena[1], Shri Krishna Mishra[2*], Anugrah Singh[2]

[1]Suresh Gyan Vihar University, Jaipur

[2]Department of Mechanical Engineering, Suresh Gyan Vihar University Jaipur

Email: rahulmeena1995m@gmail.com, krishna.mishra1187@gmail.com, anugrah.singh@mygyanvihar.com

[*]Correspondence author's email: krishna.mishra1187@gmail.com

Article Info
Volume 6, Issue 7, January 2024
Received: 17 April 2024
Accepted: 10 JUN 2024
doi:10.48047/AFJBS.6.7.2024.1991-2002

Abstract: Statistical analysis was employed to investigate heat transfer rate and thermal effectiveness of solar air heater (SAH) featuring V shaped ribs. The addition of square roughness in form of inclined ribs at a 30° angle was assessed for enhancing thermal efficiency of SAH. In the experimental setup, rib pitches of 15 mm and 20 mm were employed on upper surface of absorber plate. The heat transfer rate for 20 mm rib pitch was analyzed for comparison purposes. Several geometric characteristics of the solar duct were calculated numerically to optimize the maximum rate of heat transfer. The experimental design with a 15 mm rib pitch achieved a peak efficiency of 44.2 %, while model with a 20 mm rib pitch reached a peak efficiency of 41.4%. Both models exhibited an efficiency increase of 4.37% compared to a smooth absorber surface. First model gives the maximum absorber plate and glass cover temperatures at surface during solar intensity ranging from 1150 to 1250 W/m^2 between 12:30 PM and 1:30 PM. An exergy analysis comparison indicated that exergy value rises with increasing solar intensity throughout day. Computational Fluid Dynamics (CFD) analysis was conducted to validate the experimental findings and explored flow singularities above absorber surface.

Keywords: Irradiance of Solar; Thermal Performance; Rib Spacing; Exergy Assessment; Thermal Collector

1. Introduction

In order to do any work, a reliable and continuous energy source is needed. At now, the combustion of fossil fuels satisfies about 80% of the world's energy requirements. Nevertheless, considering

present step of use, it is anticipated that the supply of fossil fuels will be exhausted in a relatively brief period [1], [2]. An absorbent material is employed to capture the solar energy, insolation, and convert it to heat the air within the system. Solar air heating, a sustainable heating technique, can be utilized to warm or regulate air temperature. The primary areas of energy consumption for heating, particularly in commercial and industrial settings, namely space heating and industrial process heating, can significantly benefit from solar power due to its cost-effectiveness [3], [4]. This is crucial to explore and produce new replacements to fossil fuels for diminish our dependency on them. In colder regions where air heaters are commonly employed for both building heating and drying agricultural products like crops and lumber, there's an opportunity to integrate solar energy. Solar air heaters warm the incoming air as it passes through the absorber surface. However, due to relatively low heat transfer coefficient between absorber surface and air, the effectiveness of solarpowered air heaters is currently lacking [3], [5]. This phenomenon arises as result of creation of laminar sub-layer between two locations. Scientists have conducted experiments using different artificial roughness patterns in order to disturb this sub-layer and improve performance of materials. To meet the current energy demands, scientists are putting into practice the findings of a number of these studies, which have yielded the anticipated outcomes [6].

In their study, Yadav et al. [7] demonstrated a solar air heater that used wires with a roughened surface for the absorber outperformed one that used smooth wires by an 8 to 10 percent margin in terms of efficiency. Nevertheless, the improvement was not maintained until the Reynolds number surpassed 29000, suggesting that the roughened solar air heaters were not very successful in terms of thermo-hydraulic efficiency. Wang et al. [8] pursued to enhance the efficiency of solar air collectors by integrating S-shaped ribs with gaps on the surface of the absorber. Systematic experimentation demonstrated a significant enhancement in the efficiency. Anil et al. [9] discovered a association between dimensionless Nusselt number and surface absorber by creating gaps on ribs of different V-shaped artificial irregularity shapes. Using this setup, the Nusselt number experienced a 6.74-fold rise, along with a corresponding 6.37-fold increase in the friction factor, as compared to smooth plate. Patel et al. [10] examined effects of using NACA aerofoil profile for ribs in SAH, arrayed in opposite order as rough surface. The results showed a 2.53 increase in thermo-hydraulic performance at a Reynolds number of 6000. Poongavanam et al. [11] showed that solar air heaters with absorber plate surfaces had enhanced heat transfer, leading to higher Nusselt numbers compared to traditional heaters. However, this improvement is accompanied by slightly increased friction factors. Anup Kumar et al. [12] performed a statistical analysis on absorber plate of solar air heater. They determined ideal parameters to improve thermal and exergetic efficiency, which includes a relative roughness pitch of 8, a rib orientation angle of 60. Sahu et al. [13] conducted a comparison between exergy efficiency of heater with a roughness of arc-shaped wire. The results showed a significant 56 percent improvement in exergy efficiency with the rough absorber surface. Singh et al. [14] investigated the performance of solar air heaters with various roughness surfaces. They discovered that employing square wave-shaped ribs resulted in a substantial improvement in thermal-hydraulic efficiency. However, it should be noted that this enhancement came at the cost of three times greater pumping power requirements compared to a smooth absorber surface. Gawande et al. [15] estimated the efficiency of SAH that utilised a reverse L-shaped ribbed absorber surface. They achieved a thermohydraulic performance of the 1.90, with high heat transfer, by operating within specific limits of relative roughness pitch and Reynolds number. Kumar et al. [16] This triangle solar heater was tested using graphene nonmaterial imbedded in black paint to see how efficient it was in generating heat. At a speed of 1 m/s, the system's maximum efficiency is 48.23%. Manjunath et al. [17] developed turbulent air flow across the absorber surface by using spherical rib roughness. A range of Reynolds numbers was collected, ranging from 4000 to 25000. There were spherical ribs ranging from 5 to 25 millimeters in diameter. In comparison to the baseline model, the Nusselt number was found to be two times greater. Scientists came to the conclusion that the better thermal hydraulic performance provided by disc-shaped ribs. According to the literature given, there

is a lack of study that specifically investigates the long-term durability and real-world performance of solar air heaters that have roughened absorber surfaces. Although many studies have examined the short-term improvements in thermal efficiency resulting from different roughness patterns and configurations, there is a lack of research on how these improvements affect long-term efficiency during extended periods of operation and in various environmental conditions.

This research is distinctive because it thoroughly examines how V-shaped ribs with artificial roughness might improve the thermal performance of a solar air heater. While most prior research has concentrated on particular roughness configurations or restricted experimental settings, this study methodically investigates how different rib pitches and angles affect thermal efficiency. In order to maximise heat transfer rates, the study optimises the design parameters using numerical computations and statistical analysis. Lastly, a strong assessment of flow phenomena above the absorber surface is guaranteed by validating experimental data by Computational Fluid Dynamics (CFD) analysis, which increases the findings' credibility and trustworthiness.

2. Experimental Methodology

The experimental arrangement consists of a flat surface solar air heater, as depicted in Figure 1. The main body of the solar heater is a large rectangular piece made of aluminum, designed for absorption. Both the inlet and outlet lengths of experimental setup section are equal, each being 0.4 m. The outlet section of duct is connected to a pipe with a diameter of 0.053 m. The air heater is engineered to deliver a maximum solar intensity up to the 1250 W/m^2.

Gate valves at the inlet and outlet of the heater allow for adjustment of airflow. Figure 1 provides a schematic diagram of the rectangular solar air heater. Artificial roughness is introduced on the absorber surfaces using V-shaped ribs inclined at 30 degrees. One surface has a rib pitch of 15 millimeters, while the opposite surface has a pitch of 20 millimeters, as illustrated in Figure 2. An air gap separates the glass and absorber surfaces.

Before each reading session, the setup arrangement is checked for proper functioning and absence of leaks at joints. The setup is left running for at least an hour between readings to achieve steady state. Sunlight, absorber surface temperature, average glass surface temperature, pressure drop across a section, and air temperature at entry and exit sections are all recorded in each experiment of the series. There has been noticeable turbulence within the rectangular duct, and it is not anticipated that there would be any slippage at the panel of the rectangle duct component.

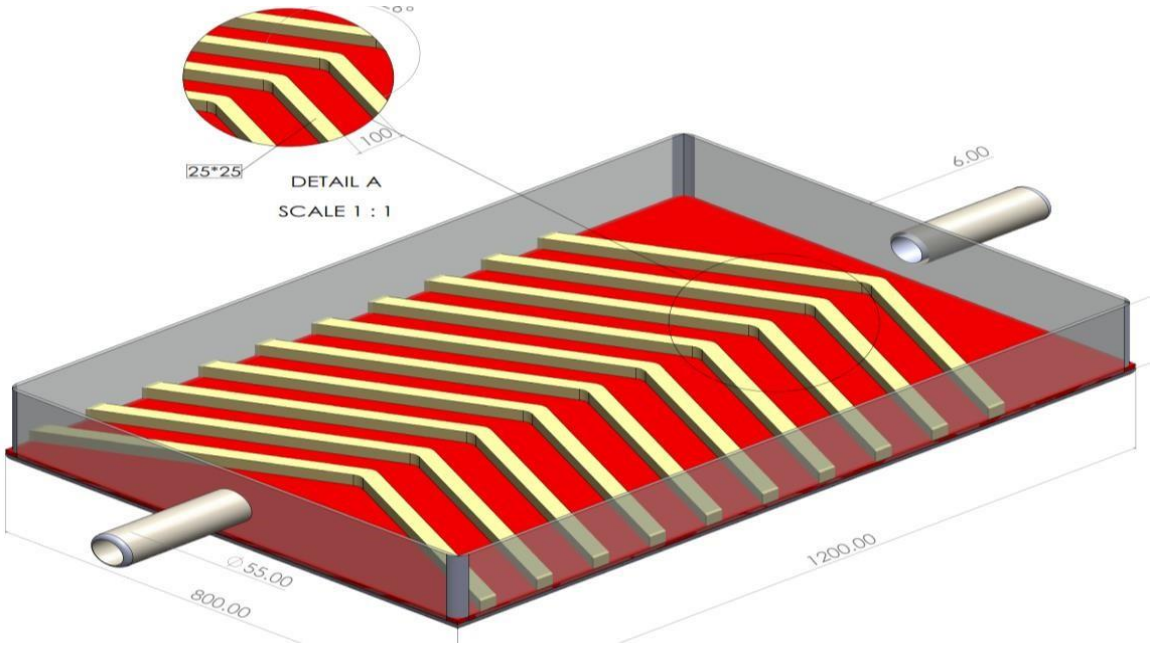

Fig. 1. Schematic diagram of rectangular solar air heater

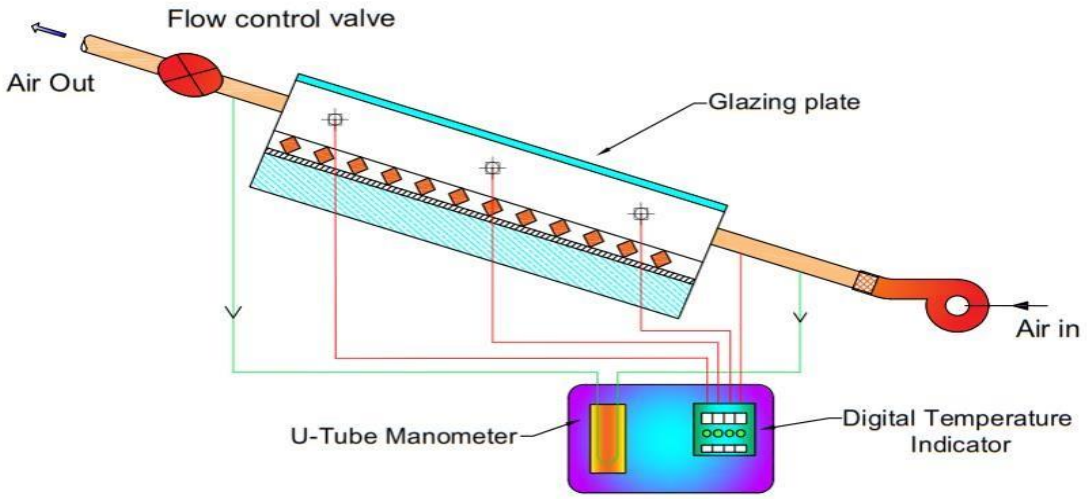

Fig. 2. Diagrammatic schematic of a rectangular solar air heater

3. Data Reduction

3.1 Efficiency Analysis

The current experimentation utilizes for V-shaped inclined ribs. Therefore, design characteristics of the heater are optimised. The efficiency of thermal has been estimated using method described below, By utilising the depicted relationship, we can approximate the overall increase in the thermal energy for the practical applications.

$$Q_{u1} = [I(\tau\alpha) - U_L(T_{pm} - T_a)]A_p$$

The calculation of mass flow rate involves the utilisation of an equation similar to the one presented,

$$\dot{m} = \frac{Q_{u1}}{C_{pa}\Delta T}$$

The flow can be determined by using the equation shown below,

$$\rho V D_H$$

$$R_e = \frac{}{\mu_a}$$

Convective heat transfer coefficients based on the Nusselt number [18],

$$N_u k_a \; h = \frac{}{D_H}$$

The equation used to compute the surface efficiency factor F' is as follows:

$$F' = \frac{}{h + hU_L}$$

The equation provides the quantification of the beneficial heat gain obtained from a solar air heater,

$$Q_{u2} = F_r[Ia(\tau\alpha) - U_L(T_{pm} - T_a)]A_p$$

$$F_r = \frac{}{A_p U_L}[1 - exp\, exp\{\frac{}{\dot{m}\, C_{pair}}\}]$$

$$\dot{m}\, C_{pair} \qquad -F' U_L A_p$$

The efficiency of system is determined using given equation,

$$\eta_{th} = \frac{Heat\ gain\ of\ Solar\ air\ heater}{The\ amount\ of\ solar\ energy\ that\ reaches\ the\ surface\ of\ the\ glass} \quad Q_u$$

$$\eta_{th} = A_p I_T$$

3.2 Analysis of Exergy

The provided equation is used to find solar air heater's exergy efficiency,

$$\eta_{ex} = 1 - \frac{\sum E_{loss}}{\sum E_{inlet}}$$

The solar air heater's net exergy energy rate is determined by,

$$\sum \dot{E}_{inlet} = IA\,[1 - \frac{4}{3}(\frac{T_a}{T_{sun}}) + \frac{1}{3}(\frac{T_a}{T_{sun}})^4]$$

The exergy destruction losses are expressed as the total of their values,

$$\sum \dot{E}_{loss} = (\dot{E}_{opt-loss}) + (\dot{E}_{q-loss}) + (\dot{E}_{fr\ -loss}) + (\dot{E}_{sun,Tp-loss}) + (\dot{E}_{Ta,Tp-loss})$$

3.3 CFD Simulation

The experimental results show that the solar air heater's increased overall efficiency is due, in part, flow state changes from the inlet to outlet. The study utilised CFD simulations in the ANSYS FLUID FLUENT and SOLIDWORKS to examine airflow dynamics between the test section's incoming air and the absorber surface with V-shaped ribs that had been roughened. Building a model and gaining comprehensive insights were both made possible by this. A more straightforward rectangular duct was made, with a bottom surface with a V-shaped, 30-degree inclined roughness geometry. Aspect ratio, or p/e ratio, was set to 2.5 for the model. The study also made use of a constant inlet velocity of 1 m/sec. Figure 3 shows the bottom-side roughness integrated model of the duct. Assuming the sun's intensity would be constant at 885 W/m^2 on April 9, 2024, at 1 p.m., given Jaipur's geographical locations.

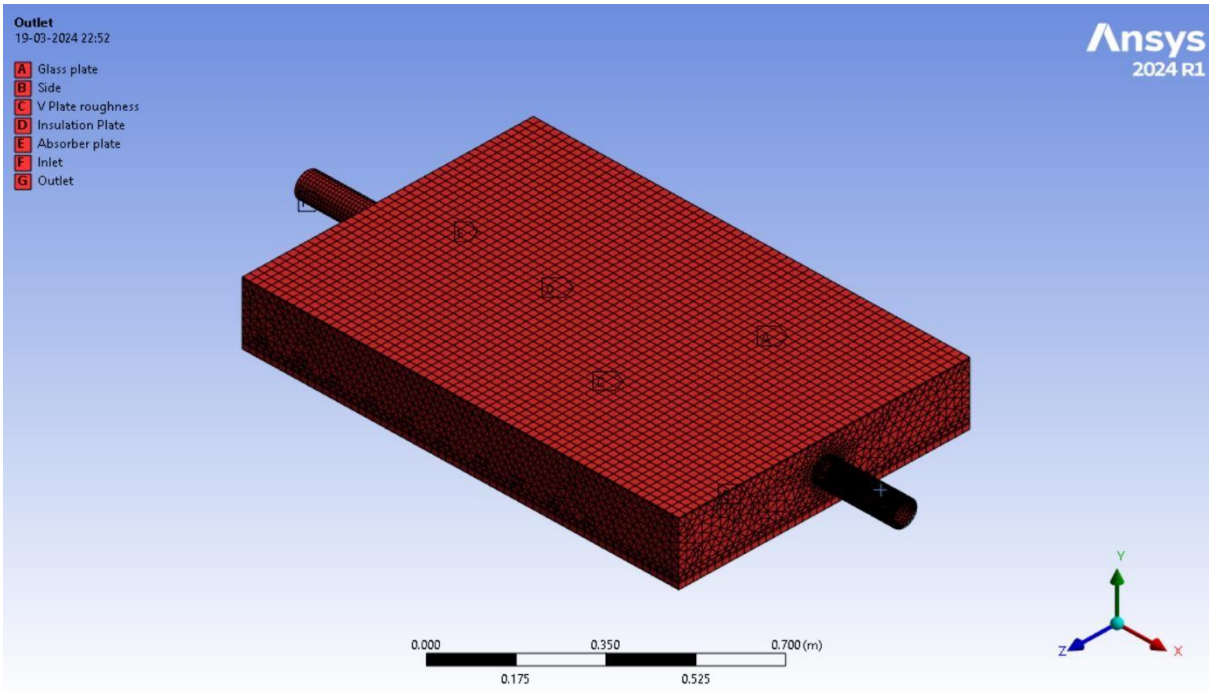

Fig. 3. Solar air heater CFD model

During the setup of CFD, it is assumed that the fluid flow is stable, incompressible, and turbulent. The channel maintains uniform fluid characteristics, with an inlet section temperature of 32^0K, at the fluid as an air at atmospheric conditions.

Figure 4 depicts procedure of generating a mesh after importing the model into Ansys Fluent. The computational domain consists of a rectangular duct with a fixed mesh size. The domain is composed of 89,766 nodes and 184,727 elements. The calculation domain utilises discrete quadrilateral grids, with a relevance set at 40 and the flexibility of choosing fine sizing.

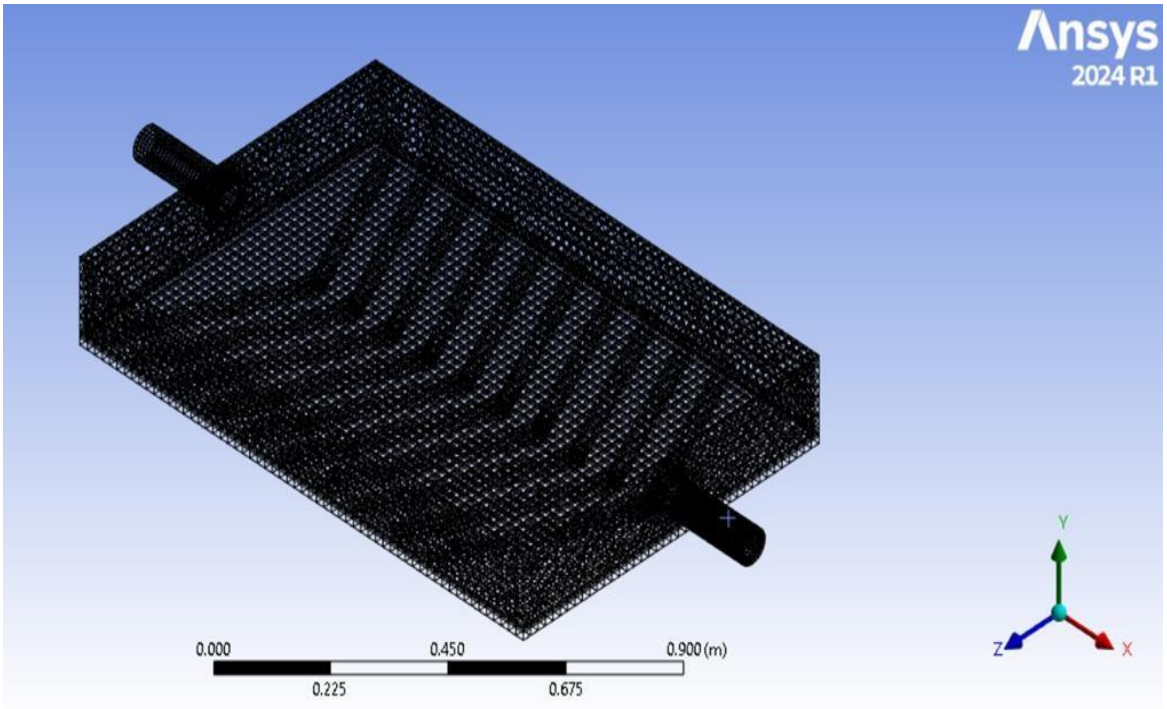

Fig. 4. Meshing arrangement of system

The absorber surface is made of aluminium, which exhibits qualities that are in line with those of materials present in Ansys library. The viscous fluid flow with increased wall treatment using the realizable k-epsilon turbulence model. The configuration of computational domain influences the Reynolds number, which in turn determines the velocity at which air enters the duct. Thus, 1 m/s is set as the velocity boundary condition at the duct's intake. The zero-gauge-pressure-outlet-function is presumptively a pressure outlet. The upper surface of the duct, in contrast to the other surfaces, undergoes a constant heat flow ranging from 850 to 1250 W/m^2.

4. Result and Discussion

4.1 Experimental Analysis

Figure 5 depicts fluctuation in the efficiency of a SAH over the course of a day. Experimental data indicates that both Model-I and Model-II achieve their maximum efficiency and performance at 1:00 PM. The Model-I has a absorber surface with a pitch of 15 mm, but Model-II has a surface with a pitch of 20 mm and V-shaped rib roughness of 30 degrees on absorber plate. The efficiency percentages for design-I and design-II are documented as follows: The percentages are as follows: 39.51%, 41.81%, 42.05%, 42.05%, 42.05%, 42.05%, 42.5%, 43.1%, 43.8%, 42.68%, and 41.39%, respectively. The intensity of solar radiation is initially very less in morning but gradually day time increases. The uppermost values, peaking at 1250 W/m^2, are observed about midday and then decrease afterwards.

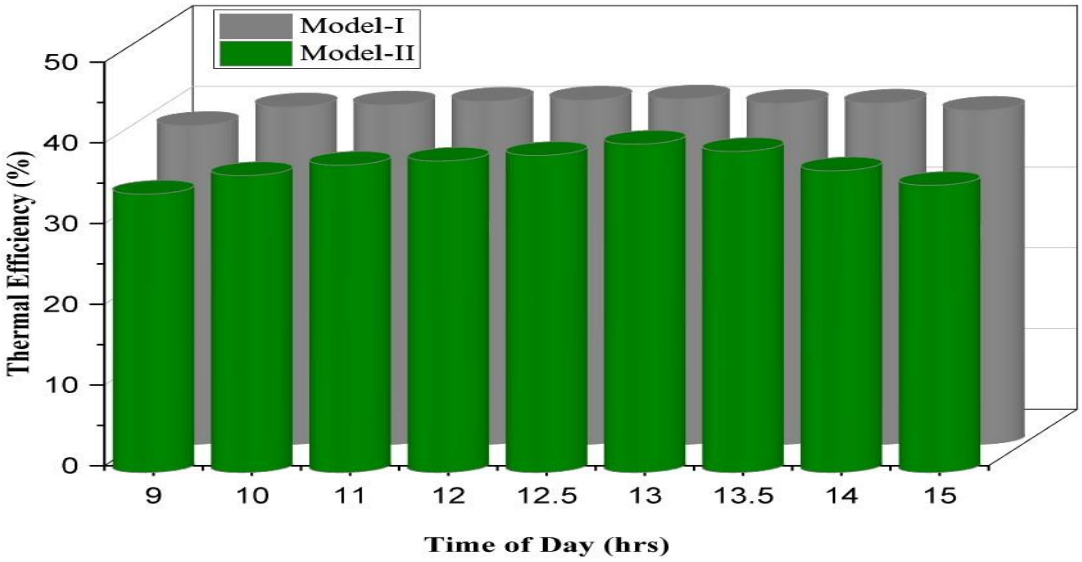

Fig. 5. SAH Thermal Efficiency vs. Time of Day

Figure 6 displays the variation in glass and absorber plate temperature over course of day for both models. These temperatures are determined using equations outlined in the calculation section. The temperatures of glazing glass and absorber plate surface are influenced by outlet and inlet section air temperatures, and it is depended on solar intensity. It is observed that Model-I exhibits higher temperatures compared to second model. This is attributed to the closer spacing of artificial rib roughness in model one, facilitating faster heat transfer between the absorber surface and the air with a larger surface area.

Additionally, Figure 7 illustrates the changes in temperature differences between the inlet and outlet sections (T0-Ti) throughout the day. The graph indicates that lower radiation intensity corresponds

to lower (T0-Ti) values. Furthermore, (T0-Ti) varies with time of day and radiation intensity, resulting in different values at different times.

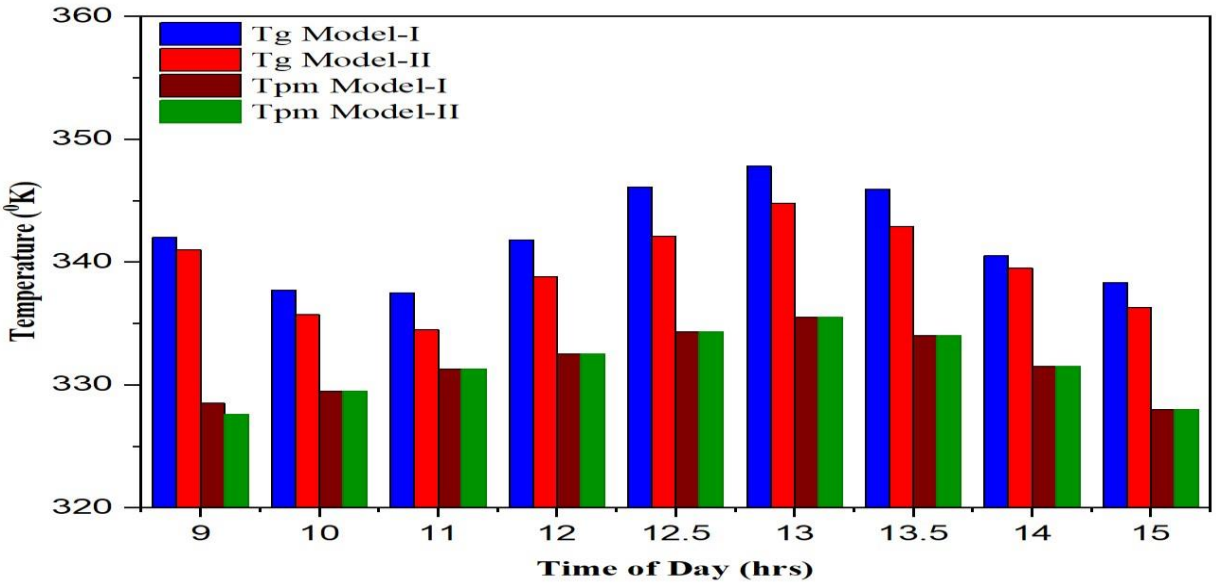

Fig. 6. Mean Absorber Surface Temperature, Glazing and SAH Time of Day

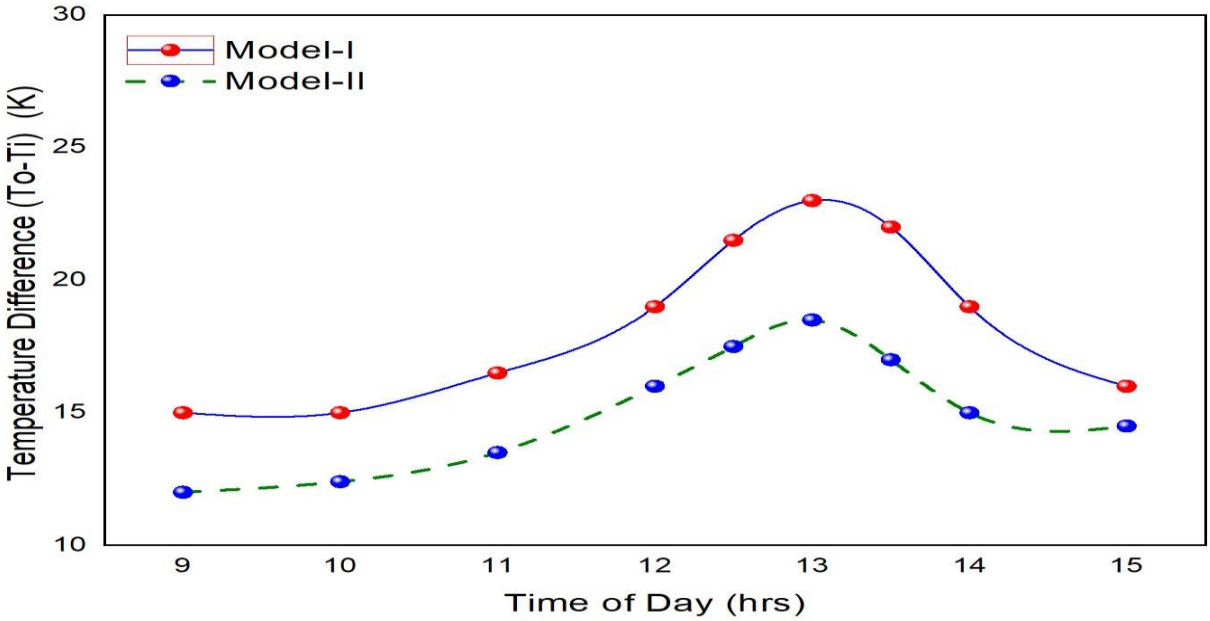

Fig. 7. Time of day vs. temperature difference (T_0-T_i)

The correlation between the passing of time and the level of radiation is shown in Figure 8. During the day of 12:30 and 1:00 p.m., the solar intensity reaches its highest point at 1250 W/m^2. The opposite is true at 9:00 a.m., when radiation intensity is 850 W/m^2. Up until 1:00 p.m., the radiation intensity steadily rises on the graph, but then it begins to fall. It's obvious that both the amount of sunlight reaching Earth and the average temperature of the Earth change over time.

Figure 9 presents a comparative analysis of solar air heater models I and II, highlighting their energy efficiency trends over the course of the day. It is observed that efficiency decreases over time in both scenarios, with a brief period where efficiency is influenced by airflow above the absorber surface, affecting heat transfer. Introducing artificial roughness to the absorber surface enhances heat transfer

rates, thereby improving heat removal rates. The temperatures at the inlet and outlet impact exergy efficiency, with both models experiencing a rise in exergy efficiency until 13:00.

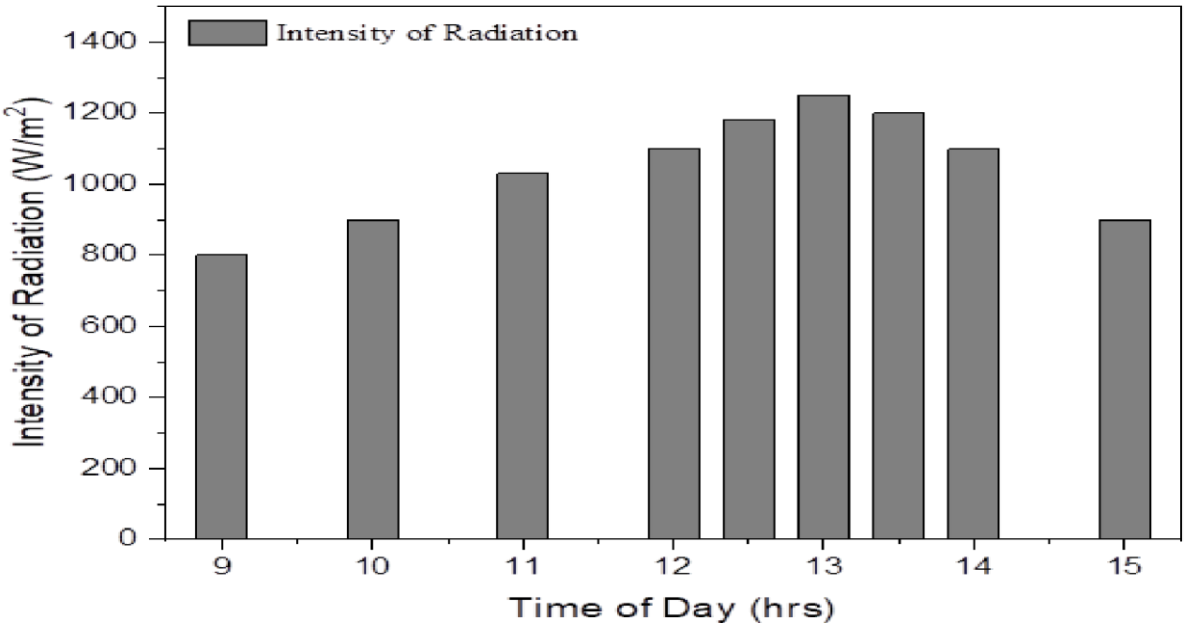

Fig. 8. Daytime and Radiation Intensity Variation

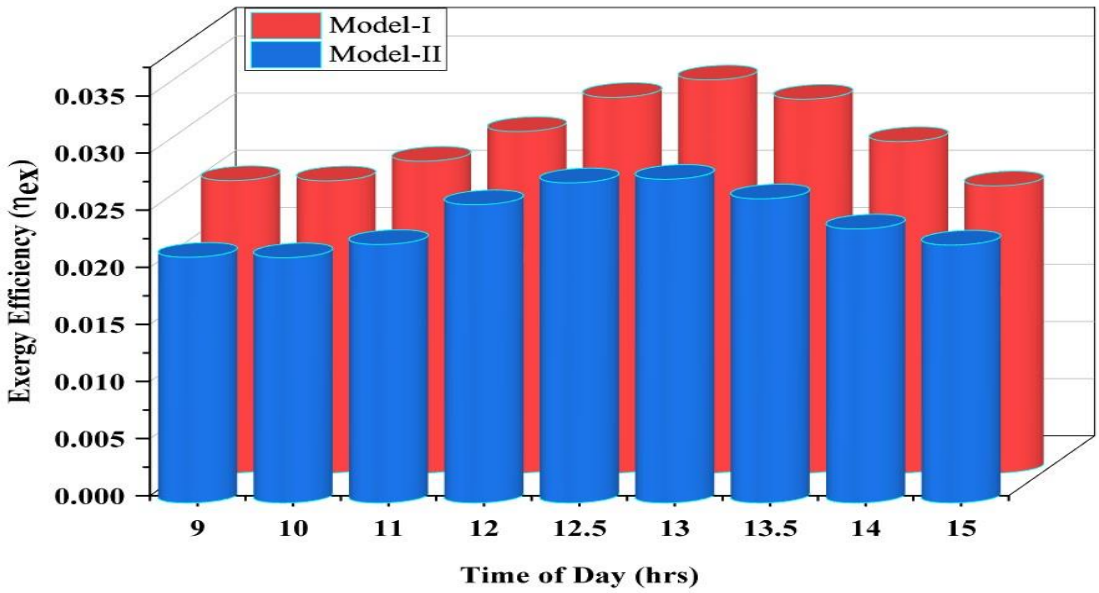

Fig. 9. The exergy Efficiency vs. Time of Day for SAH

Different kinds of loss in exergy over time are exposed in Figures 10 & 11, respectively. Out of all the loss processes, temperature difference between absorber surface and sun appears to be most significant, producing highest values for exergy loss. Its size fluctuates, reaching a maximum when the sun is very bright and a minimum when it is very dim. A solar air heater's exergy destruction losses are strongly affected by the temperature differential between its intake and output. The severity of turbulence and the pressure drop in the moving air are the factors that cause the destruction of frictional exergy. The temperature difference between the surface of absorber and moving air is reduced as convection heat transfer coefficient increases. Thus, exergy efficiency is maximized at levels of sun intensity that are higher.

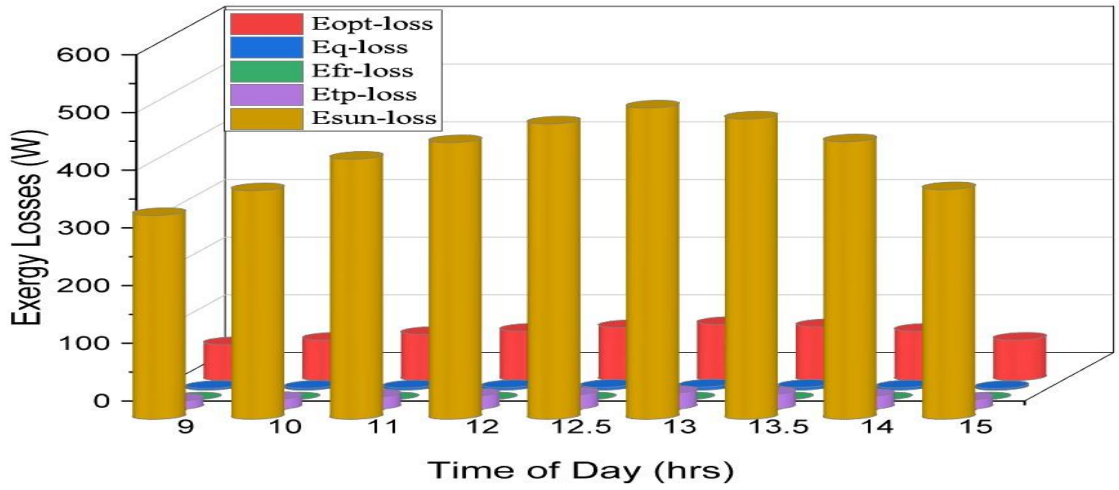

Fig. 10. Model-I Exergy Losses vs. Time of Day

The comparison of exergy efficiency between models I and II is depicted in Figure 12. Exergy efficiency is influenced by temperatures at the inlet and outlet. The peak radiation intensity of 1250 W/m^2 occurs between 12:30 and 13:00. At this solar intensity level, the solar air heater receives a higher amount of exergy energy.

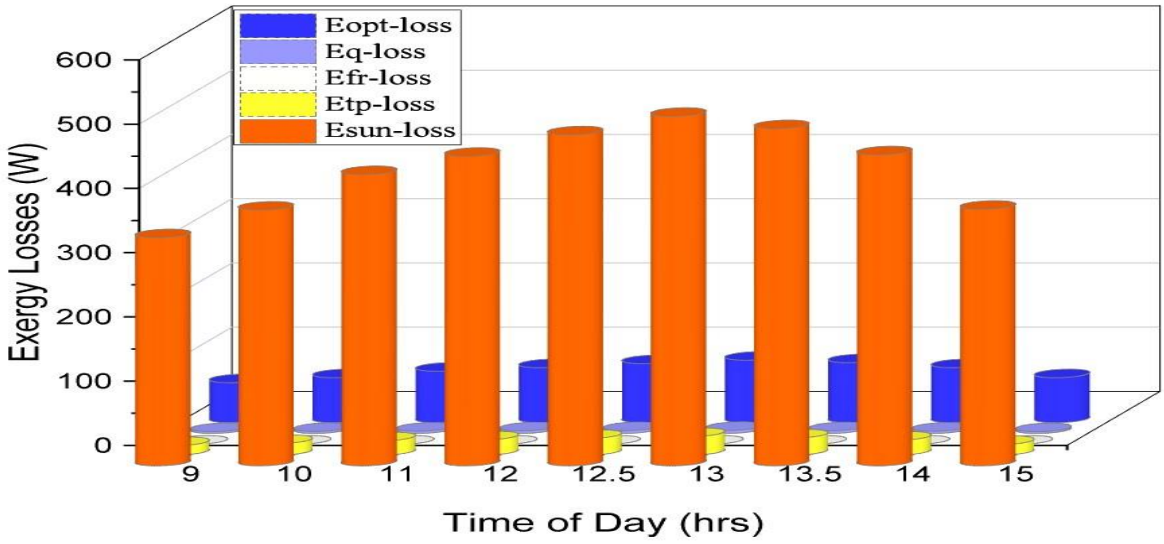

Fig. 11. Time of Day Effect on Model-II Exergy Losses

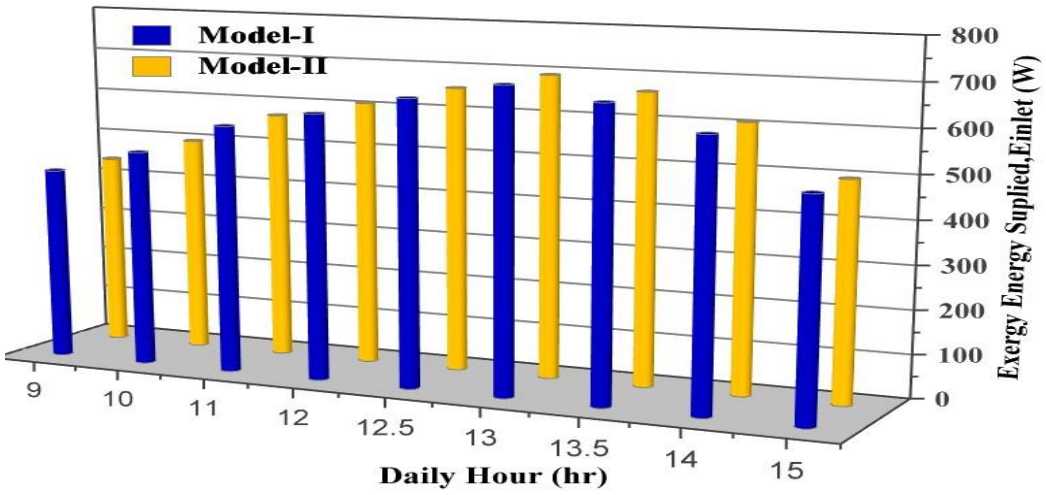

Fig. 12. SAH Exergy, Energy vs. Time of Day

5. Conclusion

The most recent experimental results show that increasing rib roughness pitch by 20 mm which increases the heat transfer rate but increases losses in friction, resulting in a decrease in total efficiency. The results of the numerical and experimental investigations of solar heater with the Vshaped roughened lead to the following findings:

- During the 9 AM to 5 PM hour, the highest efficiency for Model-I is 43.8% while for Model-II it is 40.7%.
- Rising temperatures are caused in part by the intensity of solar radiation.
- An average efficiency boost of 4.26% is achieved for the solar air heater by incorporating artificial rib roughness of 30-degree slanted V-shaped ribs.
- Sunlight intensities between 12:30 and 1:30 reach their highest points at glass covers and absorber surfaces, with temperatures ranging from 1180 to 1250 W/m^2.
- In together model, the exergy value increases when the solar intensity increases, rendering to the exergy study.
- Consistent with actual results, the CFD model shows an inlet-outlet temperature disparity of 22 K.
- According to CFD models, V-shaped with rib roughness angles of 30^0 can increase the temperature differential between the intake and outflow, leading to better pumping efficiency and less waste.

In order to improve solar air heaters' efficiency and usefulness, future research may concentrate on the following areas:

- Using sensors and algorithms, intelligent control systems are being developed to optimise temperature distribution, airflow rates, and overall system performance in response to changing environmental circumstances.
- Studies on how to combine solar air heaters with buildings' current HVAC (heating, ventilation, and air conditioning) systems to provide extra heating while lowering dependency on fossil fuels.
- Research into hybrid solar air heating systems, which combine solar power with other green energy sources or traditional heating techniques to increase performance and dependability in a range of weather scenarios.

References

[1] R. Kumar and S. Kumar Verma, “Performance estimation of Triangular Solar air heater roughened absorber surface: An experimental and simulation modeling,” Sustainable Energy Technologies and Assessments, vol. 52, p. 102208, Aug. 2022, doi: 10.1016/j.seta.2022.102208.

[2] R. Kumar, S. K. Verma, and M. Singh, “Experimental investigation of nanomaterial doped in black paint coating on absorber for energy conversion applications,” Materials Today: Proceedings, vol. 44, pp. 961–967, Jan. 2021, doi: 10.1016/j.matpr.2020.11.006.

[3] R. Kumar, S. K. Mishra, H. Kumar, R. Saxena, and A. K. Pathariya, “Experimental Investigation of Equilateral Triangle-Shaped Solar Air Heater with Two Blackened Absorber Surfaces,” in Advances in Clean Energy Technologies, P. V. Baredar, S. Tangellapalli, and C. S. Solanki, Eds., in Springer Proceedings in Energy. Singapore: Springer, 2021, pp. 221–233. doi: 10.1007/978-981-16-0235-1_19.

[4] R. Kumar, S. Verma, S. K. Mishra, A. Sharma, A. Yadav, and N. Sharma, “Performance Enhancement of Solar Air Heater using Graphene/Cerium Oxide and Graphene-Black Paint Coating on Roughened Absorber Plate,” International Journal of Vehicle Structures and Systems, vol. 14, Mar. 2022, doi: 10.4273/ijvss.14.2.23.

[5] R. Kumar and S. K. Verma, "Review based on the absorber plate coating for solar air heater applications," IOP Conf. Ser.: Mater. Sci. Eng., vol. 1116, no. 1, p. 012053, Apr. 2021, doi: 10.1088/1757-899X/1116/1/012053.

[6] T. K. Abdelkader, Y. Zhang, E. S. Gaballah, S. Wang, Q. Wan, and Q. Fan, "Energy and exergy analysis of a flat-plate solar air heater coated with carbon nanotubes and cupric oxide nanoparticles embedded in black paint," Journal of Cleaner Production, vol. 250, p. 119501, Mar. 2020, doi: 10.1016/j.jclepro.2019.119501.

[7] K. D. Yadav and R. K. Prasad, "Performance analysis of parallel flow flat plate solar air heater having arc shaped wire roughened absorber plate," Renewable Energy Focus, vol. 32, pp. 23–44, 2020, doi: https://doi.org/10.1016/j.ref.2019.10.002.

[8] D. Wang, J. Liu, Y. Liu, Y. Wang, B. Li, and J. Liu, "Evaluation of the performance of an improved solar air heater with 'S' shaped ribs with gap," Solar Energy, vol. 195, pp. 89–101, 2020, doi: https://doi.org/10.1016/j.solener.2019.11.034.

[9] A. Kumar, R. P. Saini, and J. S. Saini, "Development of correlations for Nusselt number and friction factor for solar air heater with roughened duct having multi v-shaped with gap rib as artificial roughness," Renewable Energy, vol. 58, pp. 151–163, 2013, doi: https://doi.org/10.1016/j.renene.2013.03.013.

[10] S. [Singh Patel and A. Lanjewar, "Experimental and numerical investigation of solar air heater with novel V-rib geometry," Journal of Energy Storage, vol. 21, pp. 750–764, 2019, doi: https://doi.org/10.1016/j.est.2019.01.016.

[11] G. K. Poongavanam, K. Panchabikesan, A. J. D. Leo, and V. Ramalingam, "Experimental investigation on heat transfer augmentation of solar air heater using shot blasted Vcorrugated absorber plate," Renewable Energy, vol. 127, pp. 213–229, 2018, doi: https://doi.org/10.1016/j.renene.2018.04.056.

[12] A. Kumar and A. Layek, "Energetic and exergetic performance evaluation of solar air heater with twisted rib roughness on absorber plate," Journal of Cleaner Production, vol. 232, pp. 617–628, 2019, doi: https://doi.org/10.1016/j.jclepro.2019.05.363.

[13] M. K. Sahu and R. K. Prasad, "Exergy based performance evaluation of solar air heater with arc-shaped wire roughened absorber plate," Renewable Energy, vol. 96, pp. 233–243, 2016, doi: https://doi.org/10.1016/j.renene.2016.04.083.

[14] I. Singh, S. Vardhan, S. Singh, and A. Singh, "Experimental and CFD analysis of solar air heater duct roughened with multiple broken transverse ribs: A comparative study," Solar Energy, vol. 188, pp. 519–532, 2019, doi: https://doi.org/10.1016/j.solener.2019.06.022.

[15] V. B. Gawande, A. S. Dhoble, D. B. Zodpe, and S. Chamoli, "Experimental and CFD investigation of convection heat transfer in solar air heater with reverse L-shaped ribs," Solar Energy, vol. 131, pp. 275–295, 2016, doi: https://doi.org/10.1016/j.solener.2016.02.040.

[16] R. Kumar, S. Kumar Verma, and V. Kumar Sharma, "Performance enhancement analysis of triangular solar air heater coated with nanomaterial embedded in black paint," Materials Today: Proceedings, Mar. 2020, doi: 10.1016/j.matpr.2020.02.538.

[17] M. S. Manjunath, K. V. Karanth, and N. Y. Sharma, "Numerical analysis of the influence of spherical turbulence generators on heat transfer enhancement of flat plate solar air heater," Energy, vol. 121, pp. 616–630, 2017, doi: https://doi.org/10.1016/j.energy.2017.01.032.

[18] R. Kumar, S. [Kumar Verma, and V. [Kumar Sharma, "Performance enhancement analysis of triangular solar air heater coated with nanomaterial embedded in black paint," Materials Today: Proceedings, 2020, doi: https://doi.org/10.1016/j.matpr.2020.02.538.